Available online at www.sciencedirect.com

SCIENCE DIRECT®

Ecological Modelling 178 (2004) 349–356

ECOLOGICAL MODELLING

www.elsevier.com/locate/ecolmodel

Growth dilution in multilevel food chains

Robert A. Herendeen*, Walter R. Hill

Illinois Natural History Survey, 607 East Peabody Drive, Champaign, IL 61820, USA

Received 26 June 2003; received in revised form 23 January 2004; accepted 12 March 2004

Abstract

Microalgae can absorb contaminants from the aqueous environment, and harvesting microalgae has been proposed as a method to purify water. However, rapid growth of microalgae (stimulated by increased light, for example) results in lowered tissue concentration of contaminant. This reduction has been observed to propagate to herbivores. Here we investigate (with simulation and supporting analytical argument) the propagation of growth dilution in all trophic levels of a food chain. We are concerned with concentration as well as overall mass of contaminant in each level, for different functional relationships between levels. We find that transient (i.e., prompt) growth dilution occurs for all levels. However, the new steady state concentrations can increase or decrease, depending on functional relationships (e.g., ratio versus prey dependence). These results, which have implications for pollution control, call for experimental testing.

Keywords: Growth dilution; Bioaccumulation; Biomagnification; Food chain

1. Introduction

Microalgae absorb a variety of contaminants from aquatic environments, providing a contaminated food source for higher trophic levels (Swackhamer and Skoglund, 1993; Hill et al., 1996). In rapidly growing microalgae, contaminant concentrations are reduced by the accumulation of new biomass, a phenomenon known as growth dilution. Growth dilution at the microalgal level may in principle propagate up the food chain, ultimately causing diminished contaminant concentrations in game fish and other top predators. Much quantitative analysis has been done on growth dilution in producers, e.g., Landrum et al. (1992) and Skoglund et al. (1996). Here we use simulation to investigate whether growth dilution does in fact propagate up the food chain. Because harvesting of contaminated biomass could be used as a water purification option (Sabater et al., 2002), we are concerned with overall stock of contaminant, as well as concentration, in each level.

We will assume an abruptly-occurring, constant perturbation, also called a "press" or "step-function" perturbation. We differentiate between: (1) transient dilution, the prompt response to the perturbation, and (2) steady-state dilution, i.e., the long-term response. We find that transient dilution always occurs in all levels except for extremely unlikely forms of functional dependence, but that steady state concentrations up the chain can increase or decrease depending on the functional form of feeding behavior. Thus the question of when and at what trophic level to harvest biomass to capture contaminants depends critically on functional relationships in the chain.

For example, starting with a food chain at steady state, consider the long-term response to a press

* Corresponding author. Tel.: +1-217-2442137; fax: +1-217-3336294.
E-mail address: herendee@uiuc.edu (R.A. Herendeen).

0304-3800/$ – see front matter © 2004 Published by Elsevier B.V.
doi:10.1016/j.ecolmodel.2004.03.011

doubling in light intensity. For ratio-dependent predation (i.e., a functional form that depends explicitly on the ratio of prey biomass to predator biomass) in all levels, biomass approximately doubles in every level (Herendeen, 1995), while contaminant concentrations are approximately unchanged (this is exactly true for an uncropped system). On the other hand, with Lotka–Volterra type predation in some levels, some biomass stocks change by a factor much greater than two, while others are unchanged, and concentrations in different levels can show changes of either sign (Lotka–Volterra is a limiting case of prey-dependent predation, for which the functional form depends only on on prey biomass; see Eq. (1) and discussion below it).

We first briefly discuss the functional forms we use; by simple parameter changes these can exhibit a wide range of functional dependence, including ratio-dependent and Lotka–Volterra behavior. We then present results of three simulations which demonstrate the different dilution responses with different functional dependences. Appendix A presents computational details.

2. A generalized functional form

Fig. 1 shows a food chain. All symbols are defined in Table 1. Fig. 1a shows biomass flows, and applying conservation of energy to each level gives the equations governing the dynamics (Herendeen, 1995, 2004). Fig. 1b shows the corresponding flows of contaminant. In this simple model we assume that: (1) contaminant is absorbed only by producers, passed up the food chain by predation, and exits by cropping or possibly by metabolism (Cabana et al., 1994; Futter, 1994; Rasmussen et al., 1990; Thoman, 1989; Oliver and Niimi, 1988); (2) contaminant has no influence on growth and mortality; it is merely "dragged along" by the underlying biomass dynamics; (3) contami-

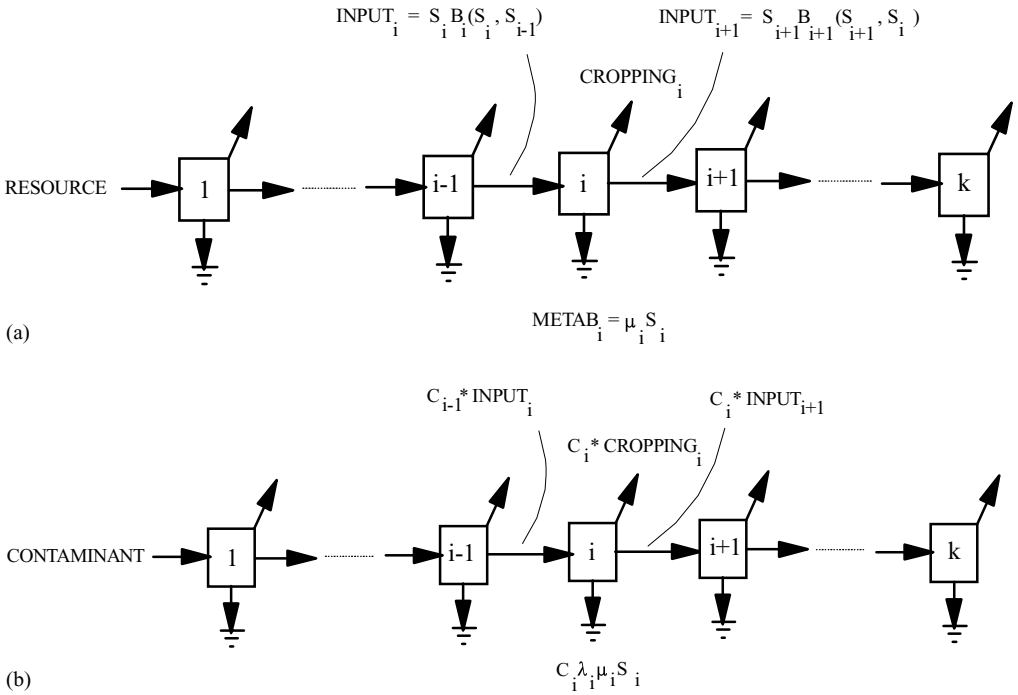

Fig. 1. Energy and contaminant flows in a food chain. All terms are defined in Table 1. Energy is expressed in grams of metabolizable biomass. Trophic level increases to the right. In the text, quantities are sometimes used with the additional subscript "0" to indicate initial values. (a) Biomass flows (unit = g(bio) per day) and stocks (unit = g(bio)). (b) Contaminant flows (unit = g(con) per day) and stocks (unit = g(con)). "Resource", e.g., light or nutrient, is assumed to affect only trophic level 1, producers.

Table 1
Symbols used in this article

Symbol	Description	Units
b_i	Time-dependent parameter in B_i; reflects, e.g., seasonal changes in predation efficiency	Dimensionless
$B_i(S_i, S_{i-1})$	Feeding input per unit biomass stock to level i as function of stocks of prey and predator	day^{-1}
c_i	Parameter in B_i; determines shape of Holling Type II dependence on prey abundance	Dimensionless
C_i	Contaminant concentration in trophic level i	g(con) g(bio)$^{-1}$
C_w	Ambient contaminant concentration	g(con) l^{-1}
CROPPING$_i$	Exogenous removal from level i; negative values indicate stocking	g(bio) day^{-1}
INPUT$_i$	Feeding input to level i	g(bio) day^{-1}
k	Number of trophic levels in food chain	Dimensionless
$k_{e,i}$	Rate constant for elimination of contaminant by level i	day^{-1}
k_w	Rate constant for uptake of contaminant by level 1 (producers)	l day^{-1} per g(bio)
METAB$_i$	Metabolic loss from level i	g(bio) day^{-1}
q_i	Parameter expressing degree of prey dependence	Dimensionless
r_i	Parameter expressing degree of interference between feeders, also called predator dependence	Dimensionless
RESOURCE$_i$	Resource (light or nutrient) intensity; affects level 1 only	Dimensionless
S_i	Biomass stock of level i	g(bio)
T_i	Contaminant stock in level i	g(con)
α_i	Relative abundance of level i's prey	Dimensionless
λ_i	Parameter expressing level i's "leakage" of contaminant via metabolism	Dimensionless
μ_i	METAB$_i$/S_i (assumed constant)	day^{-1}

g(con): grams of contaminant; g(bio): grams of biomass.

nant does not degrade internally. In Fig. 1b, $\lambda_i = 0$ corresponds to no loss and hence maximum biomagnification in level i. $\lambda_i = 1$ corresponds to no biomagnification.

Assumptions 1–3 apply well to organic forms of heavy metals (e.g., Laarman et al., 1976). The density-dependent feeding by level i on level $i-1$ is potentially a function of both levels' biomass stocks, as given in Eq. (1):

$$B_i \equiv \frac{\text{INPUT}_i}{S_i} = \frac{\text{INPUT}_{i,0}}{S_{i,0}} \frac{b_i(c_i+1)\alpha_i}{(c_i+\alpha_i)}$$

where

$$\alpha_i \equiv \text{“abundance”} \equiv \frac{(S_{i-1}/S_{i-1,0})^q}{(S_i/S_{i,0})^r} \quad (1)$$

where quantities are defined in Fig. 1. INPUT (gross primary production for producers, feeding for higher trophic levels) is assumed to have has a Holling Type II dependence on abundance. Ratio-dependent predation is defined by $q = r = 1$; prey-dependent predation, by $q = 1$, $r = 0$. Prey dependence with $c \to \infty$ is Lotka–Volterra functional dependence. b_i is potentially time-dependent (Herendeen, in press), but here is assumed constant.

3. Simulation results

Our approach can be applied to a system with any number of trophic levels, but three levels suffice to illustrate our points. Fig. 2 shows the hypothetical food chain we analyze, composed of producers,

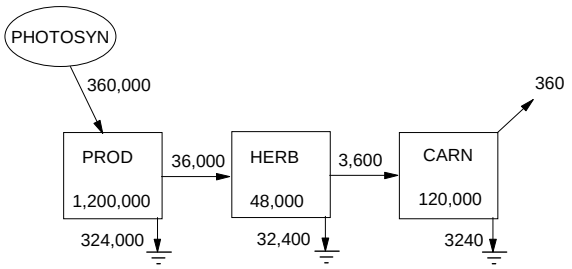

Fig. 2. Energy flows and stocks in hypothetical 3-level food chain at initial steady state, before change in light level. Numbers in compartments are biomass stocks (unit = g(bio)). Other numbers are biomass flows (unit = g(bio) per day). Levels 1, 2, and 3 are producers, herbivores, and carnivores, respectively. For each trophic level, biomass input per unit of biomass is a nonlinear function of the biomass of prey and predator. Metabolic loss is proportional to biomass stock. Cropping is determined exogenously. Production (here called input)/biomass ratios are typical of aquatic systems. Their inverses are 3.33, 1.33, and 33.33 day, for producers, herbivores, and carnivores, respectively.

herbivores, and carnivores, also called levels 1–3, respectively. The biomass flows and stocks are chosen to give production-to-biomass ratios typical of aquatic systems (Morin et al., 1999; Yurista and Schulz, 1995; Binkowski and Rudstam, 1994; Brett, 1971).

We assume that $\lambda = 0.2$, 0.2, and 0.2, respectively. By Eq. (1), this gives initial concentrations for levels 1–3 in the ratio 1:3.6:12.8, respectively (for all $\lambda_i = 0$ they would be in the ratio 1:10:100). These λs are the maximum values we infer from published data on elimination rates; see Appendix B. Our results are substantially the same for any smaller values for λ. Figs. 3–5 show simulations of this chain subjected to a abrupt doubling of the light intensity. In Fig. 3, the chain is assumed to have nonlinear ratio-dependent predation in all levels. Fig. 3a shows that biomass approximately doubles in all levels. Fig. 3b shows that contaminant concentrations exhibit transient dilution in all levels. For steady state, however, concentration remains roughly the same in levels 1 and 2 and increases by a factor of 1.16 in level 3. Thus level 3 exhibits modest steady state growth concentration, not dilution (if level 3 were uncropped, all levels would show no concentration change). Table 2 summarizes results for all simulations.

In Fig. 4, level 1 (producers) and 2 (herbivores) are assumed to have the same ratio dependence as in Fig. 3, but level 3 (carnivores) now has Lotka–Volterra predation. This combination is chosen because it

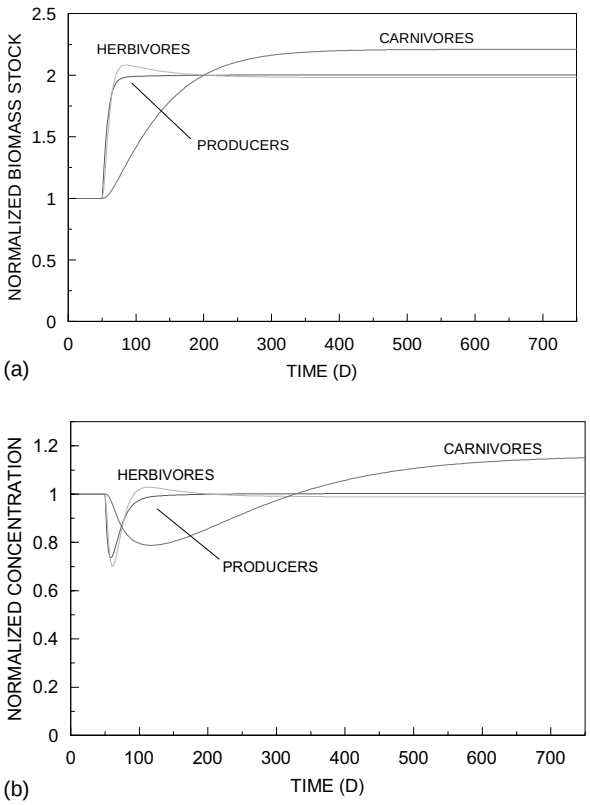

Fig. 3. Results of simulation of 3-level food chain perturbed by a doubling of light intensity at time = 50 days. All levels are assumed to have ratio-dependent predation. All quantities are normalized to unity before the light change. (a) Biomass stock; (b) contaminant concentration.

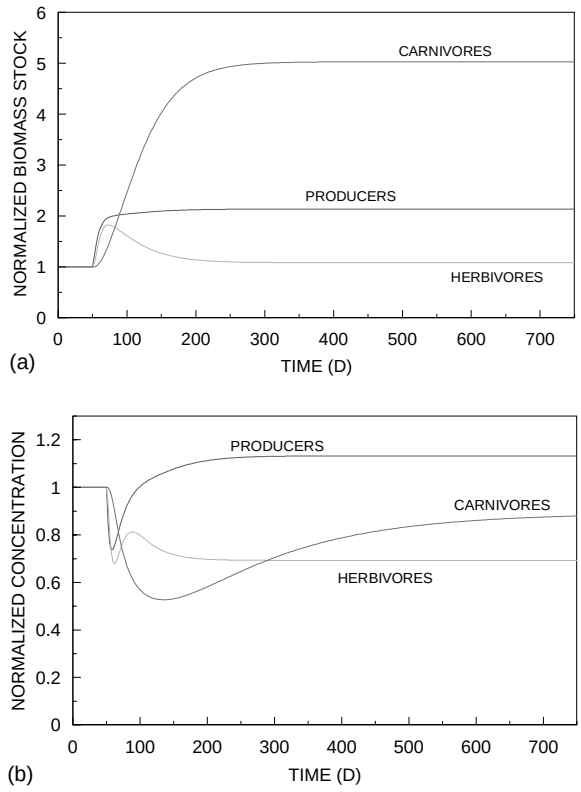

Fig. 4. Results of simulation of 3-level food chain perturbed by a doubling of light intensity at time = 50 days. Levels 1 (producers) and 2 (herbivores) are assumed to have ratio-dependent predation. Level 3 (carnivores) is assumed to have Lotka–Volterra predation. All quantities are normalized to unity before the light change. (a) Biomass stock; (b) contaminant concentration.

Table 2
Summary of steady state changes in biomass stock, contaminant concentration, and contaminant stock in three simulations of response to a doubling of light intensity

	Simulation 1	Simulation 2	Simulation 3
Level		Functional form	
1 Producers	Ratio-dependent	Ratio-dependent	Ratio-dependent
2 Herbivores	Ratio-dependent	Ratio-dependent	$c = 1$; $q = 0.03$; $r = 1$
3 Carnivores	Ratio-dependent	Lotka–Volterra	Ratio-dependent
Biomass stock (g(bio))			
1 Producers	2.00×	2.14×	2.19×
2 Herbivores	1.98×	1.08×	1.21×
3 Carnivores	2.21×	5.03×	1.26×
Contaminant concentration (g(con) (g(bio))$^{-1}$)			
1 Producers	1.00×	1.13×	1.19×
2 Herbivores	0.99×	0.69×	1.18×
3 Carnivores	1.16×	0.89×	1.25×
Contaminant stock (g(con))			
1 Producers	2.00×	2.42×	2.61×
2 Herbivores	1.96×	0.75×	1.43×
3 Carnivores	2.56×	4.48×	1.58×

g(con): grams of contaminant; g(bio): grams of biomass. '2.14×' means an increase by a factor of 2.14, etc. Ratio-dependent: $c = q = r = 1$. Lotka–Volterra: $c = 1E6$ (i.e., approximately ∞), $q = 1$, $r = 0.1$ (i.e., approximately 0). Simulation 3 mimics the "green world" hypothesis; see text. $\lambda_1 = \lambda_2 = \lambda_3 = 0.2$ for all simulations.

shows (Fig. 4b) both steady state growth concentration (level 1) and steady state growth dilution (levels 2 and 3). Fig. 4a shows that while levels 1 and 3 undergo large biomass increases, level 2 changes very little. This large–small–large pattern was described by Oksanen et al. (1981).

In Fig. 5 the functional dependence is chosen to mimic the "green world" hypothesis of Hairston et al. (1960): herbivores are unresponsive to abundance of producers, i.e., $q_2 \approx 0$. Fig. 5a bears this out; producer biomass more than doubles, but herbivore and carnivore biomass increase by only 21 and 26%, respectively. All three levels show modest steady state growth concentration (Fig. 5b).

4. Discussion

In spite of obligatory transient dilution (observed in our simulations and justified theoretically in Appendix A), the three simulations show widely differing steady state results for both concentration and total contaminant stock. The most dramatic result is the decrease in concentration, and in total contaminant, in herbivores in Simulation 2 (Fig. 4), which results from changing the functional dependence of carnivores on herbivores from a ratio-dependent to a Lotka–Volterra form. Several of the specific simulation results can be justified by analytic arguments, discussed in Appendix A.

We suggest that the possibility of such differing results should stimulate experiments of growth dilution in multilevel (>2) food chains, and that the design, analysis, and interpretation of all growth dilution experiments should pay proper attention to the effect of functional dependence.

We have not discussed the detailed form of concentration versus time in the period between the prompt growth dilution and the eventual steady-state results. We understand that for potentially valid constraints of time and other factors, experiments may be confined to the transient period. This will require much more effort in specifying and conducting experiments, and in designing models, if one wishes to draw solid quantitative conclusions. We will pursue dynamic issues in future publications.

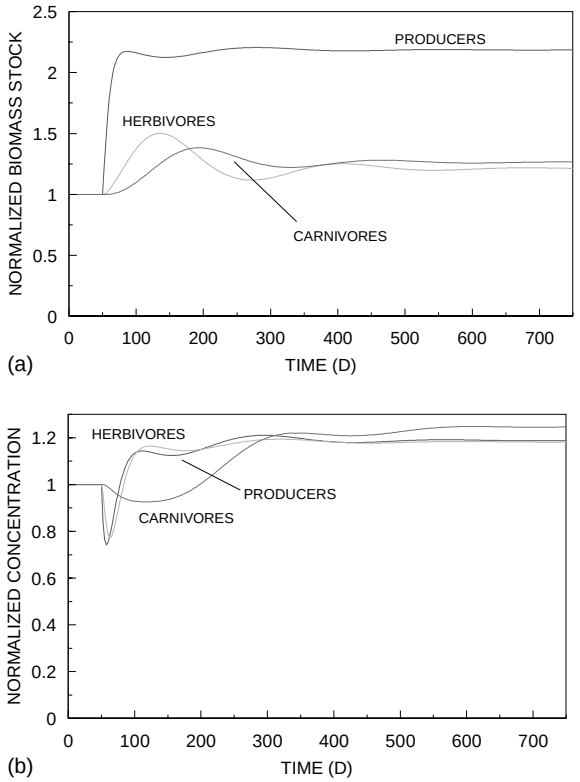

Fig. 5. Results of simulation of 3-level food chain perturbed by a doubling of light intensity at time = 50 days. "Green world" hypothesis: levels 1 (producers) and 3 (carnivores) are assumed to have ratio-dependent predation, while level 2 (herbivores) has $q = 0.03$ and $r = 0.1$. All quantities are normalized to unity before the light change. (a) Biomass stock; (b) contaminant concentration.

Appendix A. Analytical aspects of growth dilution in the model used here

The dynamics of biomass (S) and contaminant (T) stocks are indicated in Fig. 1. For each quantity, the time derivative in each level is the difference between input and output flows for that level:

$$\begin{aligned}\frac{\mathrm{d}S_i}{\mathrm{d}t} &= \mathrm{INPUT}_i - \mathrm{CROPPING}_i - \mathrm{METAB}_i \\ &\quad -\mathrm{INPUT}_{i+1} \\ \frac{\mathrm{d}T_i}{\mathrm{d}t} &= C_{i-1}\mathrm{INPUT}_i - C_i\mathrm{CROPPING}_i \\ &\quad -C_i\lambda_i\mathrm{METAB}_i - C_i\mathrm{INPUT}_{i+1} \end{aligned} \tag{A.1}$$

For level 1, producers, Eq. (A.1) is modified as follows. For $\mathrm{d}T_1/\mathrm{d}t$, the first term is replaced by $C_\mathrm{w}k_\mathrm{w}S_1$, where C_w is the ambient concentration and k_w is a constant. For the first term in $\mathrm{d}S_1/\mathrm{d}t$, S_{i-1} is interpreted as the resource level, which here means the light level.

$C_i = T_i/S_i$. Differentiating the concentration gives:

$$\begin{aligned}\frac{\mathrm{d}C_i}{\mathrm{d}t} &= \frac{1}{S_i}\frac{\mathrm{d}T_i}{\mathrm{d}t} - \frac{T_i}{S_i^2}\frac{\mathrm{d}S_i}{\mathrm{d}t} \\ &= C_{i-1}\frac{\mathrm{INPUT}_i}{S_i} - \frac{C_i}{S_i}(\mathrm{INPUT}_i - (1-\lambda_i)\mu_i S_i)\end{aligned} \tag{A.2}$$

Neither cropping nor predation appears in Eq. (A.2), because neither directly changes concentration. At steady state the time derivative is zero. Solving Eq. (A.2) in that case gives:

$$\begin{aligned}\frac{C_i}{C_{i-1}} &= \frac{(\mathrm{INPUT}_i/S_i)}{(\mathrm{INPUT}_i/S_i) - (1-\lambda_i)\mu_i} \\ &= \frac{B_i}{B_i - (1-\lambda_i)\mu_i}\end{aligned} \tag{A.3}$$

For level 1, Eq. (A.3) has the form

$$C_1 = \frac{C_\mathrm{w}k_\mathrm{w}}{B_1 - (1-\lambda_1)\mu_1} \tag{A.4}$$

Eq. (A.3) shows that $C_i/C_{i-1} = 1$ for $\lambda_i = 1$: with 100% leakage there is no biomagnification.

Observation 1. Eq. (A.2) *shows that transient growth dilution, as exhibited in* Figs. 3b, 4b, and 5b, *will always occur with a growth-stimulus to level* 1, *producers. To see this, differentiate* Eq. (A.2) *with respect to prey*:

$$\frac{\partial}{\partial S_{i-1}}\left(\frac{\mathrm{d}C_i}{\mathrm{d}t}\right) = (C_{i-1} - C_i)\frac{\partial B_i}{\partial S_{i-1}} \tag{A.5}$$

Starting with a steady state in which biomagnification already occurs, $C_{i-1} - C_i < 0$. Eq. (1) *then shows that* $\partial B_i/\partial S_{i-1} > 0$, *as long as* $q > 0$. *Then the right hand side of* Eq. (A.5) <0. *Because* $\mathrm{d}C_i/\mathrm{d}t = 0$ *at steady state, this means* $\mathrm{d}C_i/\mathrm{d}t$ *becomes negative, defining growth dilution.*

Observation 2. *For steady state,* Eq. (A.3) *gives the magnification factor. With an ecological efficiency of* 10% *and* $\lambda = 0$, *the factor is* 10. *Biomass stocks*

Table B.1
Calculated values of λ from published values for k_e

Reference	Contaminant	Organism	k_e (per day)	Trophic level	μ (per day)	$\lambda = k_e/\mu$
Hill and Larsen, unpublished	Hg (inorganic)	Periphyton	0.048	1	0.27	0.18
Skoglund et al. (1994)	PCBs	Phytoplankton	0.0003–0.09	1	0.27	0.001–0.3
Trudel (1980)	Hg	Daphnia	0.14	2 (herbivore)	0.675	0.21
Headon et al. (1996)	Hg	Crayfish	0.0	2 (herbivore/ omnivore)	0.675	0.0
Fowler et al. (1978)	Hg	Marine shrimp	0.0013	2 (omnivore)	0.675	0.0019
Miettinen et al. (1972), Fowler et al. (1978)	Hg	Mussel	0.0007–0.011	2 (herbivore)	0.675	0.001–0.016
Huckabee et al. (1975)	Hg	Mosquito fish	0.0	3 (planktivore)	0.027	0.0
Trudel and Rasmussen (1997)	Hg	Rainbow trout	0.0013–0.0026	3	0.027	0.048–0.096
Trudel and Rasmussen (1997)	Hg	Northern pike	0.0009–0.005	3	0.027	0.03–0.2

μ is calculated from the model system in Fig. 2.

and inputs (flows) change according to the functional forms and the effect of perturbations to resource and cropping; details are in Herendeen (1995, 2004).

As one example, we can relate an observed concentration increase to the changes in biomass when the light is doubled. In Table 2, Simulation 2, we see a factor of 1.13 increase in concentration in level 1, producers, even as producer biomass increases by a factor of 2.14. This apparently surprising result can be justified by reference to Eq. (A.4). $\lambda_1 = 0.2$. All quantities are constants except B_i; what happens to it when resource (i.e., light) doubles and S_1 increases by a factor of 2.14? Eq. (1) shows that B_1 decreases; light is now less abundant given that $q = r = 1$ for level 1. Then the denominator of Eq. (A.4) decreases and C_1 increases. One can verify the magnitude of the change, given initial values of $B_1 = 0.3$ per year and $\mu_1 = 0.27$ per year, obtained from Fig. 2.

Appendix B. Relating the model leakage factor, λ, to observed elimination rates, k_e

The standard experiment to measure k_e is the logical equivalent of that used by Headon et al., 1996 which is summarized as follows. Prey (or ambient, for producers) containing radioactively labeled contaminant is offered to the target organism, resulting in contaminant accumulation. Measurements begin when unlabeled but otherwise identical prey (or ambient) are then offered. One obtains total count rate from the target organism over time (correcting for the half-life of the tracer) and fits it to an exponential: (count rate) = (count rate)$_0$ $\exp(-k_e t)$.

We can relate this experiment to our model using Eq. (A.1), noting that the experimental conditions dictate that there is no input of labeled contaminant, no cropping, and no predation:

$$\begin{aligned}\frac{dT_{i,\text{labeled}}}{dt} &= -C_{i,\text{labeled}}\lambda_i \text{METAB}_i \\ &= -C_{i,\text{labeled}}\lambda_i\mu_i S_i \\ &= -\lambda_i\mu_i C_{i,\text{labeled}} S_i = -\lambda_i\mu_i T_{i,\text{labeled}}\end{aligned} \tag{B.1}$$

Eq. (B.1) describes exponential decay of total labeled contaminant: $T_{i,\text{labeled}} = T_{i,\text{labeled},0}\ \exp(-\lambda_i\mu_i t)$. Hence $\lambda_i = k_{ei}/\mu_i$. In Table B.1 we list calculated values for λ based on published values of k_e. For self-consistency, we use only the Hg results. For trophic levels 1–3, we see that the maximum λ is approximately 0.2.

References

Binkowski, F.P., Rudstam, L.G., 1994. Maximum daily ration of Great Lakes bloater. Trans. Am. Fisheries Soc. 123, 335–343.

Brett, J.R., 1971. Satiation time, appetite, and maximum food intake of sockeye salmon (*Oncorhynchus nerka*). J. Fisheries Res. Board Can. 28, 409–415.

Cabana, G., Tremblay, A., Kalff, J., Rasmussen, J.B., 1994. Pelagic food chain structure in Ontario lakes: a determinant of mercury levels in lake trout (*Salvelinus namaycush*). Can. J. Fisheries Aquat. Sci. 51, 381–389.

Fowler, S.W., Heyraud, M., La Rosa, J., 1978. Factors affecting methyl and inorganic mercury dynamics in mussels and shrimp. Mar. Biol. 46, 267–276.

Futter, M.N., 1994. Pelagic food-web structure influences probability of mercury contamination in lake trout (*Salvelinus namaycush*). Sci. Total Environ. 145, 7–12.

Hairston, N., Smith, F., Slobodkin, L., 1960. Community structure, population control, and competition. Am. Nat. 94, 421–425.

Headon, C.M., Hall, R.J., Mierle, G., 1996. Dynamics of radiolabelled methylmercury in crayfish (*Orconectes virilis*). Can. J. Fisheries Aquat. Sci. 53, 2862–2869.

Herendeen, R., 1995. A unified quantitative approach to bottom-up:top-down and trophic cascade hypotheses. J. Theor. Biol. 176, 13–26.

Herendeen, R., 2004. Bottom-up and top-down effects in food chains depend on functional dependence: an explicit framework. Ecol. Model. 171, 21–33.

Herendeen, R., in press. Dynamic trophic cascade. Ecol. Model.

Hill, W.R., Stewart, A.J., Napolitano, G.E., 1996. Mercury speciation and bioaccumulation in lotic primary producers and primary consumers. Can. J. Fisheries Aquat. Sci. 53, 812–819.

Huckabee, J.W., Goldstein, R.A., Janzen, S.A., Woock, S.E., 1975. Methylmercury in a freshwater food chain. In: Proceedings of the International Conference on Heavy Metals in the Environment, Toronto, Ontario, pp. 199–215.

Laarman, P., Willford, W., Olson, J.R., 1976. Retention of mercury in the muscle of yellow perch (*Perca flavescens*) and rock bass (*Ambloplites rupestris*). Trans. Am. Fisheries Soc. 105, 296–300.

Landrum, P., Lee, H., Lydy, M., 1992. Toxicokinetics in aquatic systems: model comparisons and use in hazard assessment. Environ. Toxicol. Chem. 11, 1709–1725.

Miettinen, J.K., Heyraud, M., Keckes, S., 1972. Mercury as a hydrospheric pollutant. II. Biological half-time of methyl mercury in four Mediterranean species: a fish, a crab, and two molluscs. In: Ruivo, M. (Ed.), Marine Pollution and Sea Life. Fishing News Ltd., London, UK, pp. 295–298.

Morin, A., Lamoureux, W., Busnarda, J., 1999. Empirical models predicting primary productivity from chlorophyll a and water temperature for stream periphyton and lake and ocean phytoplankton. J. North Am. Benthol. Soc. 18 (3), 299–307.

Oksanen, L., Fretwell, S., Arruda, J., Nielema, P., 1981. Exploitation of ecosystems in gradients of primary productivity. Am. Nat. 118, 240–261.

Oliver, B.G., Niimi, J., 1988. Trophodynamic analysis of polychlorinated biphenyl congeners and other chlorinated hydrocarbons in the Lake Ontario ecosystem. Environ. Sci. Technol. 22, 388–397.

Rasmussen, J.B., Rowan, D.J., Lean, D.R.S., Carey, J.H., 1990. Food chain structure in Ontario Lake determines PCB levels in lake trout (*Salvelinus namaycush*) and other pelagic fish. Can. J. Fisheries Aquat. Sci. 47, 2030–2038.

Sabater, S., Guasch, H., Romani, A., Munoz, I., 2002. The effect of biological factors on the efficiency of river biofilms in improving water quality. Hydrobiologica 469, 149–156.

Swackhamer, D.L., Skoglund, R.S., 1993. Bioaccumulation of PCBs by algae: kinetics versus equilibrium. Environ. Toxicol. Chem. 12, 831–838.

Skoglund, R.S., Swackhamer, D.L., 1994. Fate of hydrophobic organic contaminants. In: Baker, L.A. (Ed.), Environmental Chemistry of Lakes and Reservoirs. American Chemical Society, Washington, DC, USA, pp. 559–573.

Skoglund, R., Stange, K., Swackhamer, D., 1996. A kinetics model for predicting the accumulation of PCBs in phytoplankton. Environ. Sci. Technol. 30, 2113–2120.

Thoman, R.V., 1989. Bioaccumulation model of organic chemical distribution in aquatic food chains. Environ. Sci. Technol. 23, 699–707.

Trudel, B.K., 1980. Studies of mercury bioaccumulation by *Daphnia magna* Straus with a model for simulating whole animal pollutant accumulation, Ph.D. thesis. University of Ottawa, Ottawa, Ontario, Canada.

Trudel, M., Rasmussen, J.B., 1997. Modelling the elimination of mercury by fish. Environ. Sci. Technol. 31, 1716–1722.

Yurista, P.M., Schulz, K.L., 1995. Bioenergetic analysis of prey consumption by *Bythotrephes cederstroemi* in Lake Michigan. Can. J. Fisheries Aquat. Sci. 52, 141–150.